EUROPEAN ORGANIZATION FOR NUCLEAR RESEARCH

Proposal to the ISOLDE and Neutron Time-of-Flight Committee

The $^{14}N(n,p)^{14}C$ and $^{35}Cl(n,p)^{35}S$ reactions at n_TOF-EAR2: dosimetry in BNCT and astrophysics.

[submission date: 30/05/2017]

J. Praena[1], I. Porras[1], M. Sabaté-Gilarte[2,3], F. Ogállar[2,1], P. Torres-Sánchez[1], , C. Lederer-Woods[4], T. Davinson[4], M. Dietz[4], S.J. Lonsdale[4], P.J. Woods[4], M. Barbagallo[5], J. Andrzejewski[8], J. Perkowski[8], S. Cristallo[9,10] for the n_TOF collaboration and

C. Abia[6], F. Arias de Saavedra[1], I. Domínguez[6], B. Fernández[3,7], M. Macías[3,7]

[1] Departamento de Física Atómica, Molecular y Nuclear, Universidad de Granada, Spain.
[2] European Organization for Nuclear Research (CERN), Switzerland.
[3] Departamento de Física Atómica, Molecular y Nuclear, Universidad de Sevilla, Spain
[4] School of Physics and Astronomy, University of Edinburgh, United Kingdom.
[5] Istituto Nazionale di Fisica Nucleare, Sezione di Bari, Italy.
[6] Departamento de Física Teórica y del Cosmos, Universidad de Granada, Spain.
[7] Centro Nacional de Aceleradores (US-CSIC-JA), CNA, Sevilla, Spain.
[8] University of Lodz, Poland.
[9] INFN, Sezione di Perugia, Italy.
[10] INAF, Osservatorio Astronomico di Teramo, Teramo (Italy).

Spokesperson(s): Javier Praena (jpraena@ugr.es)
Marta Sabaté-Gilarte (marta.sabate.gilarte@cern.ch)
Claudia Lederer-Woods (claudia.lederer-woods@ed.ac.uk)

Technical coordinator: Oliver Aberle

Abstract

Nitrogen and Chlorine are present in the human body and the $^{14}N(n,p)^{14}C$ and $^{35}Cl(n,p)^{35}S$ reactions are of key importance in the boron neutron capture therapy of cancer because the emitted protons deliver locally a relevant dose in tissue. Their contribution in the ^{10}B-loaded is much lower than the dose produced by ^{10}B, but they crucially contribute to the dose in healthy tissue which is the limiting factor in whatever radiotherapy treatment. In nuclear astrophysics, the $^{14}N(n,p)$ reaction plays an important role as neutron poison as it absorbs neutrons available for capture on elements in the slow process. Also it may have a relevant role in the origin of ^{19}F, still matter of debate. The $^{35}Cl(n,p)$ reaction is involved in the creation of ^{36}S, whose astrophysical origin remains unresolved, as well as is matter of debate the observed deviation from the solar $^{35}Cl/^{37}Cl$ ratio in recent observations in carbon-rich AGB stars. The existing experimental data preclude us from reliably determining the role of these reactions in the mentioned fields. In both reactions, protons of low energies are emitted (~590 keV) which makes that experiment challenging, but perfectly suited for a measurement at EAR-2 which exhibits the highest instantaneous neutron flux worldwide, efficiently suppressing background not related to the neutron beam. This proposal is a continuation of the Letter of Intent (CERN-INTC-2014-007/INTC-I-156) which aims to improve the capabilities of the n_TOF facility making it suitable for (n,p) measurements for low energy protons.

Requested protons: $3{,}5 \cdot 10^{18}$ protons on target
Experimental area: EAR-2

1. SCIENTIFIC MOTIVATIONS

1.1 Dosimetry in Neutron Capture therapy

Boron Neutron Capture Therapy (BNCT) is an experimental radiotherapy that makes use of low energy neutrons and has produced recently very promising clinical results in cancer of very bad prognosis [1]. It consists of the injection of a ^{10}B carrier, with high tumour-cell specificity, and the subsequent irradiation of the tumour area with neutrons. Neutrons are moderated by the tissue and reach the boron doped-tumour with thermal energy. After the reaction with ^{10}B, an α-particle (1.47 MeV) and ^{7}Li nucleus (0.8 MeV) are ejected and produce strong damage in the cell while sparing nearby ones because their range in tissue is of the order of the cell size. Clinical trials have been only performed in nuclear research reactors mainly for the treatment of glioblastoma and recurrent head and neck cancers [1]. The development of low energy and high current proton and deuteron accelerators is pushing a new era in BNCT due to the construction of accelerator-based facilities (AB-BNCT) that has attracted a renewable interest of the IAEA in BNCT [2]. The current figure-of-merits (FOM) were published by the IAEA [3], and at present a group is in charge of writing a new Technical Document (TECDOC) for BNCT in which new FOMs will be defined, therefore, the nuclear data used for reference dosimetry calculations are under review and upgrade. The International Commission on Radiation Units and Measurements (ICRU) recommends that the delivered dose should have less than 5% deviation from the prescribed dose [4].

In clinical trials, the dose delivered to a ^{10}B loaded tumour due to $^{10}B(n,\alpha)^{7}Li$ is more than four times higher than the sum of all the others reactions [5]. However, the delivered dose to the healthy tissue is the limiting factor. The quantity that takes into account the proportion of an isotope and its cross-section versus the energy is the kerma factor. The neutron kerma factor is due to neutron-induced reactions without photon emission. Figure 1 shows the reference dosimetry calculations of neutron kerma factors for brain (healthy) tissue [6]. Although the presence of brain tissue of N (2.2%) and Cl (0.3%) is much lower than other elements their importance is much higher. In other tissues, as the skin, the ICRU models have a double concentration of N than in brain [7].

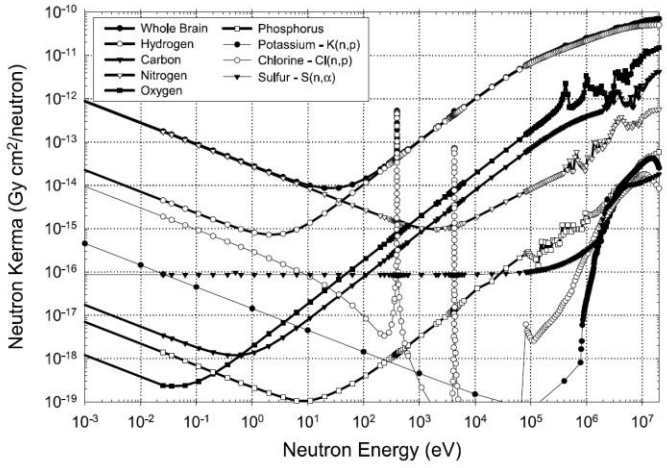

Figure 1. Contributions of the different elements to the neutron kerma for an adult whole brain. All kerma is from ICRU 63, except K, Cl and S which were calculated for the dominant reactions using ENDF/B-VI or JENDL-3.2 cross-sections. "Reference Dosimetry Calculations for Neutron Capture Therapy with Comparison of Analytical and Voxel Models", Med. Phys. 29, 145-56 (2002). J. T. Goorley, Medical Physics 29, 2 February 2002 [6]. These calculations performed with ENDF/B-VII.1 provide the same conclusions.

1.2 Nuclear astrophysics.

Elements heavier than Fe are created mainly by successive neutron captures and beta decays, either during He-burning in Red Giant stars by slow(s)-process or Supernovae or Neutron Star Mergers by rapid(r)-process. Nevertheless, neutron induced reactions on lighter nuclei may be of key importance for heavy element abundances produced in the s-process, as they may act as "neutron poison", i.e., absorbing neutrons and thereby decreasing neutrons available for capture on the heavy isotopes. The $^{14}N(n,p)^{14}C$ reaction represents an important neutron poison reaction, as the ^{14}N available at the s-process sites may consume a large fraction of neutrons [8]. In addition, $^{14}N(n,p)^{14}C$ is involved in the creation of ^{19}F, whose astrophysical origin is still matter of debate [9][10], as it provides protons for the ^{19}F production, via the

chain of reactions $^{18}O(p,\alpha)^{15}N(\alpha,\gamma)^{19}F$. ^{19}F is a useful tracer of the physical conditions in stellar interiors because it can be easily destroyed by proton and alpha reactions, therefore any production mechanism also has to enable ^{19}F to escape from the hot stellar interiors after its production as demonstrate the observed high abundance in AGB atmospheres [11][12]. In addition to this, recently, important discrepancies as high as 100% between experimental Maxwellian averaged cross-sections (MACS) and $^{14}N(n,p)$ evaluations have been found [13].

The $^{35}Cl(n,p)^{35}S$ reaction influences the synthesis of the rare isotope, ^{36}S, whose origin remains unresolved [14]. Recently, observations of the circumstellar envelope of carbon-rich AGB stars have shown first evidence of a significant deviation from solar isotopic ratio of heavier elements ($^{35}Cl/^{37}Cl$) than the CNO cycle [15]. Current discrepancies in the MACS and gaps at certain stellar energies preclude us from reliably determining the role of the $^{35}Cl(n,p)^{35}S$ reaction on ^{36}S abundances and deviation of the solar isotopic ratio.

2. STATUS OF THE DATA.

2.1 $^{35}Cl(n,p)^{35}S$ reaction.

Figure 2 (left) shows the data available in EXFOR (points) and the last ENDF-VII evaluation [16] (line) which is mainly based on Koehler [17] who measured from thermal to 100 keV. In the resonances, the evaluation is based on Druyts *et al.* [18] that only provided the cross-section for each resonance (measured at GELINA) and the thermal point (measured at ILL). Few concerns were shown in [16]: the resonances of Druyts *et al* [18] could be only fitted using the thermal value of Koehler [17] (12% higher than Druyts), and for this reason the evaluation did not take into account other thermals values as that of Gledenov *et al.* [19] (23% higher than Koehler [17]); in any case, as the evaluation claimed [16], the resonances were poorly fit. Figure 2 (right), taken from [16], shows the resonance at 27 keV as a representative example of the quality of the fit with SAMMY code [20] (line) of the experimental data (points) of Druyts *et al* [18].

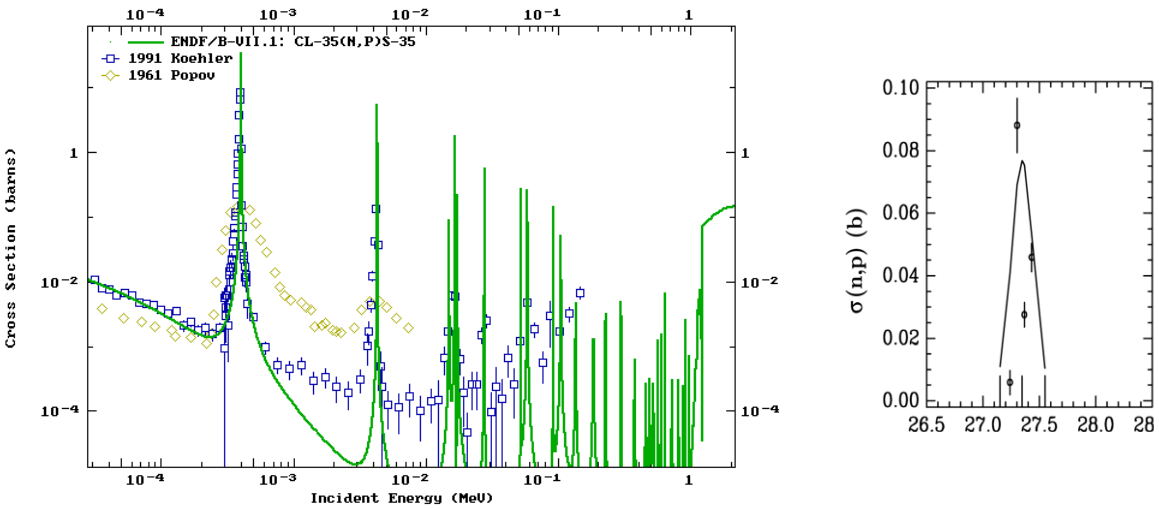

Figure 2. Left: ENDF/B-VII.1 (line) in comparison with the data in EXFOR (points) for the $^{35}Cl(n,p)$ cross-section. Right: experimental points of the resonance at 27 keV in comparison with the fit achieved with SAMMY [16].

The evaluation discussed and determined the resonance parameters for three experimental data set [17], [18] and [19] showing significant differences in the strengths of the 0.398 and 4.25 keV resonances, the most important ones, and relevant discrepancies for other resonances. Druyts *et al.* [18] also compared their data with Koehler [17], showing that even though the normalization performed of both dataset, important discrepancies remained in the resonance strengths and in the MACS. As mentioned in Druyts *et al.* the latter was related to the normalization to different thermal values which has a direct impact on MACS values [18]. In the resonance region, Druyts *et al.* justified the differences to Koehler not only because their higher resolution but also due to the assumption of isotropic emission in Koehler's analysis.

At n_TOF-EAR2 we will provide data from thermal to MeV region in a unique measurement enabling a better understanding the role of the $^{35}Cl(n,p)^{35}S$ reaction in BNCT and astrophysics. The proposed setup, Section 4, will allow measuring the cross section independently of the proton emission wave character.

2.2 $^{14}N(n,p)^{14}C$ reaction.

There is a fair amount of experimental data on $^{14}N(n,p)^{14}C$, with cross section spanning over several different energy ranges. However, the existing discrepancies are important and relevant for dosimetry and astrophysics. From 61 meV to 35 keV, there is only one differential measurement, Koehler and O'Brien [8], therefore the evaluations are based on it, but its extrapolation to thermal energy does not match the most recent results of Wagemans *et al.* [21] (Fig. 3, inset). The possible deviation of a factor ~2 at thermal has important consequences in BNCT because the crucial importance of the $^{14}N(n,p)^{14}C$ reaction on the delivered dose to healthy tissue (Figure 1). Between 35 and 150 keV, an important region for astrophysics, there is no differential cross-section data and only spectrum-average (SPA) cross-sections and MACS exist. These measurements must to assume the cross-section dependency on the energy in order to obtain their values. Gledenov *et al.* [22] measured SPA at kT= 25, 53 and 144 keV obtaining a constant value, in good agreement with Koehler *et al.* [8] at 25 keV, but a factor 2.5 and 4 higher than Brehm *et al.* [23] for the MACS at kT=25 and 53 keV, respectively.

Recently, Wallner *et al.* [13] measured the MACS at kT=25 keV, obtaining a value 11% discrepant with the evaluation (JEFF-3.2), and at kT=123 and kT=178 keV a factor 2 discrepant to JEFF-3.2 and also to the data of Johnson *et al.* [24] (Fig. 3). In particular, the calculated MACS at kT=100 keV in [13] is 100% lower than the JEFF-3.2 evaluation. Wallner *et al.* suggested that the discrepancies originate from the significant influence of the resonance at 493 keV in the cross-section at much lower energies; therefore this resonance should be precisely determined. From 150 keV to the 493-keV resonance, Johnson *et al.* [24] (Fig. 3, yellow points) is the only measurement and their data show significant discrepancies with the evaluations and [13]. Later, Morgan [25] (Fig. 3, blue points) measured the cross-section and obtained a lower strength of the 493-keV resonance than Johnson. Following this trend, Wallner *et al.* [13] have proposed a further reduction of a factor 3.3 of the 493-keV resonance strength of Morgan [25]. It can be noticed that the evaluations are based on Morgan for the 493-keV resonance.

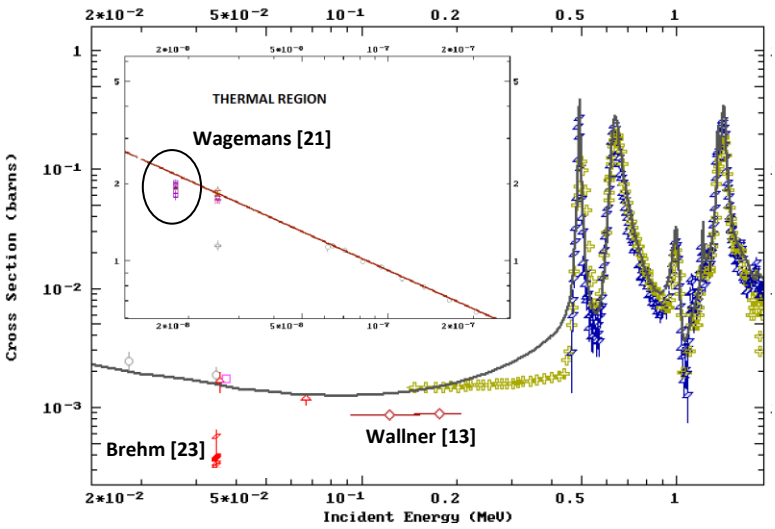

Figure 3. Experimental data of the $^{14}N(n,p)^{14}C$ cross-section available in EXFOR (points) in comparison with JEFF-3.2 (line) from 20 keV to 2 MeV. Grey points correspond to Koehler [8], yellow points to Johnson [24], blue points to Morgan [25], the rest of points correspond to SPA or MACS values discussed in the text. It can be noticed although, the discrepancies in the 493-keV resonance between Johnson *et al.* [24] and Morgan [25], they match in the description of the 635-keV resonance.
The inset corresponds to the thermal region; line corresponds to the JEFF-3.2 evaluation and points to experimental data being [21] the most recent ones.

At n_TOF-EAR2, for the first time, it can provide more reliable data from thermal to the MeV region in a unique measurement completing the gap and lack of cross-section data. This will enable a better understanding the role of the $^{14}N(n,p)^{14}C$ reaction in BNCT and astrophysics.

3. THE RESULTS OF THE LoI: samples and Micromegas detectors.

In the LoI [26] we aimed to prepare a setup for improving the capabilities of the n_TOF facility making it suitable for (n,p) reactions for low energy protons in a wide energy range. A compromise between thin sample, enough count rate and good separation of the signals of low energy protons from the noise and background was required. Part of this work was carried out during M. Sabaté-Gilarte´s PhD thesis at CERN [27], in particular the enhancement of the ratio signal to noise at EAR2 by means of in-beam Micromegas (MGAS) detectors. Previously to the test of the LoI, ^{35}Cl and ^{14}N samples were made by evaporation in vacuum of KCl and Adenine, respectively, onto 16-μm thick Al backings. Similar techniques were used for performing the samples used in the experiments [8], [17] and [18]. However, a study of the homogeneity or the dependency of the mass with the radius (r) was not carried out [8, 17, 18, 28]. We have characterized one of our KCl samples by Rutherford Backscattering Spectrometry (RBS) with α-beam at CNA (Spain). This has revealed an r^2 dependency of the mass thickness with r. An average value of number atoms of ^{35}Cl in our sample is $1.1 \cdot 10^{-6}$ at/b. Concerning ^{14}N samples, the mass of adenine (~200 μg/cm^2) was determined by the difference in the mass before and after the evaporation onto Al backing. All the samples will be carefully characterized by RBS. Figure 4 shows the TOF spectra obtained with MGAS detectors (90% Ar + 10% CF_4) at EAR2 for the ^{14}N(n,p)^{14}C and ^{35}Cl(n,p)^{35}S reactions with ~10^{17} protons. It can be noticed that it is possible to resolve the resonance at 398 eV of the ^{35}Cl(n,p)^{35}S reaction, demonstrating the feasibility of both measurements with the proposed setup.

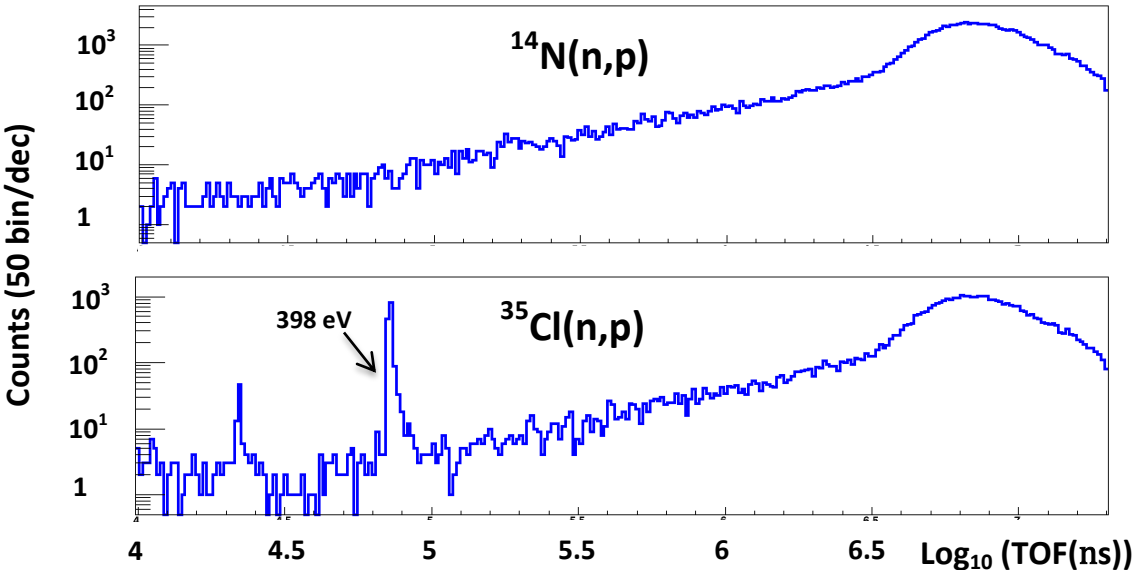

Figure 4. Time-of-flight spectra in the same scale and energy range measured at n_TOF-EAR2 with MGAS detectors for ^{14}N(n,p)^{14}C (top panel) and ^{35}Cl(n,p)^{35}S (bottom panel) reactions for approximately 10^{17} protons.

4. SETUP. COUNTS FOR 3e18 PROTONS.

The most important part of the setup (Figure 5, left) will consist of 3 MGAS chambers: a first one with two MGAS detectors for one ^{235}U and one ^{10}B sample as reference standards, a second chamber with two MGAS detectors for two Nitrogen samples in back-to-back configuration, and a third chamber with two MGAS detectors for two Chlorine samples in back-to-back configuration. The MGAS setup will be in-beam with an almost 2π geometric efficiency per sample (2π back and 2π forward) and with no dependence of the efficiency on emission angle.

Downstream, another chamber with two off-beam DSSSD detectors (40μm thickness, 5cmx5cm, 16x16 strips) and one Cl and one N sample will be placed. The DSSSDs will provide information on a possible

anisotropy of the emitted protons in the most important resonances by taken advantage of the position sensitivity provided by the strips.

We have estimated the counts for the **MGAS detectors at EAR2** with ENDF/B-VII.1 data for both reactions and the samples mentioned in section 3. Figure 5 (right) shows the estimation of counts for both reactions for 80 bins per decade (bpd) with $3 \cdot 10^{18}$ protons. For the $^{14}N(n,p)^{14}C$ reaction we reach the goals: a wide energy range from thermal to the MeV region, good statistics and well resolved first and second resonances. For the $^{35}Cl(n,p)^{35}S$ reaction, we will also provide data in a large energy range from thermal to the MeV region, resolving resonances and with very good statistics in the most important ones.

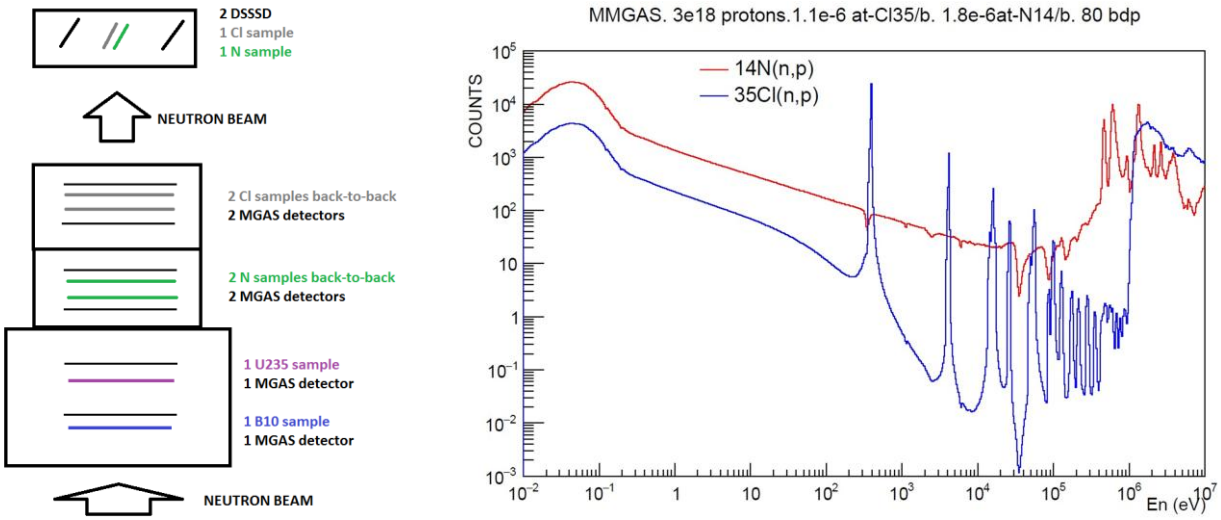

Figure 5. Left: sketch of the setup. Right: estimation of the number of counts for $^{14}N(n,p)^{14}C$ (read line) and $^{35}Cl(n,p)^{35}S$ (blue line) reactions considering the MGAS setup, the mass of the samples already performed, $3 \cdot 10^{18}$ protons on target and the ENDF/B-VII.1 cross-sections.

4. CONCLUSIONS

We propose to measure the $^{14}N(n,p)^{14}C$ and $^{35}Cl(n,p)^{35}S$ cross-sections in a wide energy range, from thermal to MeV region, for the first time. In addition to this, in case of $^{14}N(n,p)^{14}C$ reaction, our experiment aims: to provide differential cross-section data from 35 to 150 keV for the first time, to measure the resonance at 493 keV (discrepant descriptions are available) which has a very important effect at lower energies and to provide a thermal value as accurate as possible. Concerning $^{35}Cl(n,p)^{35}S$ reaction, our experiment also aims: to provide resonance data with high energy resolution and better statistics, a better description of the resonances with SAMMY and a value at thermal energy more compatible with the description of the rest of the cross-section.

In BNCT of cancer both reactions are important because their crucial contribution to the dose in healthy tissue. The data for these reactions should be very accurate (5%) and the new generation of AB-BNCT, for which neutron beams will be slightly different from reactor beams, requires of new and more accurate data than available at present. This is particular important for dose in healthy tissue of the brain where the concentration of Cl tissue is higher than in the rest of the body, and in the healthy tissue of the skin, for which ICRU models have double concentration of N than in the rest of the body. In astrophysics we will study the role of ^{14}N as neutron poison and its influence in the creation of ^{19}F. Also we can provide new information on the origin of Cl, isotopic ratio $^{35}Cl/^{37}Cl$, and its role in the production of ^{36}S. The obtained data at n_TOF-EAR2 facility will considerably improve the quality of the available data and will allow solving or clarifying the questions under debate mentioned through the text.

We request 3.5e18 protons: <u>0.5e18 for detector calibration</u> with reference samples and fine tune of the parameters of the detectors (thresholds and gains); and **<u>3e18 for the cross-section measurement</u>** in order to have 5% uncertainty in the significant neutron energy regions with a low energy resolution for ~20 bpd, and 5-10% uncertainty in the resonances with a high energy resolution. Both experiments are suitable to run in parallel for an optimization of the number of protons.

References

[1] NUPECC, Report *Nuclear Physics for Medicine* (2014). http://www.nupecc.org/pub/npmed2014.pdf

[2] https://www.iaea.org/newscenter/news/boron-neutron-capture-therapy-back-in-limelight-after-successful-trials

[3] IAEA-TECDOC-1223, *Current status of neutron capture therapy*, May 2001.

http://www-pub.iaea.org/MTCD/publications/PDF/te_1223_prn.pdf

[4] ICRU Rep. 46, International Commission on Radiation Units and Measurements, Bethesda, MD, (1992).

[5] L. Kankaanranta, T. Seppala, H. Koivunoro *et al., L-boronophenylalanine-mediated boron neutron capture therapy for glioblastoma or anaplastic astrocytoma progressing after external beam radiation therapy : A Phase I study.* Int. J. Radiat. Oncol. Biol. Phys. 80, 369-376 (2011).

http://www.redjournal.org/article/S0360-3016%2810%2900323-8/abstract

[6] J.T. Goorley, W.S. Kiger III, R.G. Zamenhof., *Reference Dosimetry Calculations for Neutron Capture Therapy with Comparison of Analytical and Voxel Models*, Med. Phys. 29, 145-56 (2002).

[7] ICRU 1978 Dose Specification for Reporting External Beam Therapy with Photons and Electrons ICRU Report 29 (Bethesda, MD: ICRU).

[8] P. E. Koehler *et al.*, "*^{14}N(n,p)^{14}C cross section from 61 meV to 34.6 keV and its astrophysical implications"*, Phys. Rev. C, 39, 1655 (1989).

[9] A. Renda *et al.*, "On the origin of fluorine in the Milky Way", Mon. Not. R. Astron. Soc. 354, 575-580 (2004).

[10] A. Jorissen *et al., "Fluorine in red giant stars: evidence for nucleosynthesis"s*, Astron. Astrophys. 261, 164-187 (1992).

[11] H. Jönsson *et al.*, "*Fluorine in the solar neighborhood: no evidence for the neutrino process*", The Astrophysical Journal, 835:50 (6pp), 2017.

[12] C. Abia *et al.*, "*The origin of fluorine: abundances in the AGB carbon stars revisited*", Astronomy&Astrophysics 581, A88 (2015).

[13] A. Wallner *et al., "Accelerator mass spectrometry measurements of the ^{13}C(n,γ) and ^{14}N(n,p) cross sections"*, Phys. Rev. C 93 045803 (2016).

[14] H. Schatz *et al.*, "*Stellar cross sections for ^{33}S(n,α)^{30}Si, ^{36}Cl(n,p)^{36}S and ^{36}Cl(n,α)^{33}P and the origin of the ^{36}S*", Physical Review C, volume 51, number 1, page 379 (1995).

[15] C. Kahane *et al.*, "*Improved isotopic ratio determinations in IRC+10216, the progenitor mass and the s process*", Astron. Astrophysics 357, 669-676 (2000).

[16] R.O. Sayer *et al., "R-matrix analysis of Cl neutron cross sections up to 1.2 MeV",* Phys. Rev. C 73, 044603 (2006).

[17] P. E. Koehler, *^{35}Cl(n,p) cross section from 25 meV to 100 keV,* Phys. Rev. C 44 1675 (1991).

[18] S. Druyts *et al., Determination of the ^{35}Cl(n,p) reaction cross section and its astrophysical implications,* Nucl. Phys. A537 (1994) 291-305.

[19] Y. M. Gledenov *et al.*, Joint Institute for Nuclear Research, Communication P3-89-351, Dubna, USSR, 1989 (unpublished).

[20] N. M. Larson, Tech. Rep., ORNL/TM-9179/7, 2006.

[21] J. Wagemans *et al.*,"*Experimental determination of the ^{14}N(n,p)^{14}C reaction cross section for thermal neutrons*", Phys. Rev. C 61, 064601 (2001).

[22] Yu.M. Gledenov *et al.*,"*Cross sections of the ^{14}N(n,p)^{14}C reaction at 24.5, 53.5 and 144 keV",* Z. Phys. A 348, 199-200 (1994).

[23] K. Brehm *et al., "The cross section of ^{14}N(n,p)^{14}C at stellar energies and its role as a neutron poison for s-process nucleosynthesis",* Z. Ohys. A 330, 167 (1988).

[24] C.H. Johnson and H.H Barschall, "*Interaction of fast neutrons with Nitrogen",* Phys. Rev. 80, 818 (1950).

[25] G. L. Morgan, "*Cross sections for the ^{14}N(n,p$_0$), (n,α$_0$) and the (n,α$_1$) reactions from 0.5 to 15 MeV",* Nucl. Science and Eng. 70 163-176 (1979).

[26] J. Praena, M. Sabaté-Gilarte *et al.,* for the n_TOF collaboration, "*SiMon and Micromegas tests for (n,p) measurements at n_TOF: ^{35}Cl(n,p)^{35}S and ^{14}N(n,p)^{14}C Cross Sections".* CERN-INTC-2014-007 / INTC-I-156.

[27] J. Praena, M. Sabaté-Gilarte *et al.,* for the n_TOF collaboration," *^{33}S(n,α) cross-section measurement at n_TOF EAR2",* CERN-INTC-2015-038 ; INTC-P-442. – 2015.

[28] R. Eykens *et al., "Preparation and characterization of ^{35}Cl and ^{36}Cl samples for (n,p) cross section measurements",* Nucl. Ins. And Methods in Phys. Research A303 (1992) 152-156.